Available online at www.sciencedirect.com
ScienceDirect
Journal of the European Ceramic Society 28 (2008) 35–40
www.elsevier.com/locate/jeurceramsoc

Effects of Cu and Zn co-doping on the electrical properties of $Ni_{0.5}Mn_{2.5}O_4$ NTC ceramics

Chunhua Zhao [a], Biyun Wang [a], Pinghua Yang [a], Louis Winnubst [a,b], Chusheng Chen [a,*]

[a] *Laboratory of Advanced Functional Materials and Devices, Department of Material Science and Engineering, University of Science and Technology of China, Hefei, Anhui 230026, China*
[b] *Inorganic Membranes, Faculty of Science and Technology and MESA+ Institute, University of Twente, P.O. Box 217, 7500 AE Enschede, The Netherlands*

Received 12 February 2007; received in revised form 4 June 2007; accepted 15 June 2007
Available online 21 August 2007

Abstract

The effects of Cu and Zn co-doping on Ni–Mn–O spinel-structured NTC ceramics were investigated. Dense Cu and Zn co-doped $Ni_{0.5}Mn_{2.5}O_4$ spinel-structured ceramics were prepared from mixed oxalate-derived powders. XPS analysis revealed that in the co-doped material $Cu_xZn_{1.0}Ni_{0.5}Mn_{1.5-x}O_4$, the majority of Cu ions resided at the B-sites due to the almost exclusive occupation of Zn ions at the A-sites, but in the material doped with Cu alone, Cu ions were situated at both A- and B-sites. The co-doped material exhibited a significant decrease in electrical resistivity without much decrease in the thermal constant. In comparison with the material doped with Cu alone, the co-doped material also showed much improved electrical stability upon annealing at 150 °C in air, which is attributed to its stable distribution of cations in the spinel.

Keywords: Spinels; XPS; Electrical properties; NTC; $Zn(Cu, Ni, Mn)_2O_4$

1. Introduction

Negative temperature coefficient (NTC) thermistors are thermally sensitive resistors whose resistance decreases with increasing temperature. There is a large choice of NTC materials, and the mostly used materials are Ni- and Mn-based spinel oxides of general formula AB_2O_4 such as Cu–Ni–Mn–O, Ni–Mn–O and Fe–Ni–Mn–O.[1–3] In the spinel, oxide ions are cubic close packed and cations are situated at the tetrahedral (A) and octahedral (B) sites. The electrical conduction in the spinel oxides is generally described by a small polaron hopping mechanism. The specific resistivity of these ceramics follows the well known Arrhenius relation: $\rho = \rho_0 \exp(E_a/kT)$, in which ρ is the specific resistivity, E_a the activation energy, k the Boltzmann's constant and T is the absolute temperature. Two parameters are used to characterize NTC thermistor materials, $\rho_{25\,^\circ C}$, the specific resistivity at 25 °C, and B ($=E_a/k$), the thermal constant (unit in K) which is a measure of the sensitivity of the device over a given temperature range.

There is a demand for NTC thermistors with low electrical resistance and acceptable stability. It has been found that the doping of Cu to the Mn-based spinel oxide leads to a sharp decrease in the electrical resistivity, but unfortunately at the expense of the stability.[4] There have been some studies conducted on these Cu-doped systems in terms of the valence and site occupancy of cations and electrical conduction mechanism. Based on the X-ray diffraction (XRD) studies on powders of $Mn_{2.6-x}Co_{0.4}Cu_xO_4$, Legros et al. suggested a cationic distribution $(Mn_{0.6-x}{}^{2+}Co_{0.4}{}^{2+}Cu_x{}^{+})_A[Mn_{2-x}{}^{3+}Mn_x{}^{4+}]_BO_4{}^{2-}$ for $0 \le x \le 0.6$, and $(Co_{0.4}{}^{2+}Cu_{0.6}{}^{+})_A[Cu_{x-0.6}{}^{2+}Mn_{2.6-2x}{}^{3+}Mn_x{}^{4+}]O_4{}^{2-}$ for $0.6 \le x \le 1$.[5] They further suggested that the occupation of Mn^{3+} and Mn^{4+} cations on the B-sites forms small polaron pathways, but did not take into account the effect of Cu ions per se on the electrical conduction process. By using powder neutron diffraction, thermogravimetric measurements and XPS spectroscopy analysis, Elbadraoui et al. arrived at the following cationic distribution $(Mn_{0.616}{}^{2+}Cu_{0.360}{}^{2+}Cu_{0.024}{}^{+})_A[Ni_{0.660}{}^{2+}Mn_{0.604}{}^{3+}Mn_{0.710}{}^{4+}Cu_{0.026}{}^{2+}]_BO_4{}^{2-}$ for $Cu_{0.41}$

* Corresponding author. Tel.: +86 551 3601592; fax: +86 551 3601592.
E-mail address: ccsm@ustc.edu.cn (C. Chen).

0955-2219/$ – see front matter © 2007 Elsevier Ltd. All rights reserved.
doi:10.1016/j.jeurceramsoc.2007.06.007

$Ni_{0.66}Mn_{2.93}O_4$, and proposed that Cu^{2+} ions at the A-sites take part in the electron conduction process.[1]

It has also been shown that the substitution of part of Mn by Zn in nickel manganites can improve the stability of the spinel structure against oxidation reaction.[6] Therefore, the effects of Cu and Zn co-doping are examined in this paper. XRD and XPS measurement were used to determine the valence and site occupancy of cations, and the electrical properties of the materials were investigated in relation to the distributions of cations.

2. Experimental

The mixed oxalate precursors for $Cu_xZn_{1.0}Ni_{0.5}Mn_{1.5-x}O_4$ and $Cu_xNi_{0.5}Mn_{2.5-x}O_4$ were prepared using the solid-state coordinate reaction method.[2] Analytical grade nickel acetate $Ni(CH_3COO)_2{\cdot}4H_2O$, manganese acetate $Mn(CH_3COO)_2{\cdot}4H_2O$, copper acetate $Cu(CH_3COO)_2{\cdot}H_2O$, zinc acetate $Zn(CH_3COO)_2{\cdot}2H_2O$ and oxalic acid were used as starting materials. A mixture of these acetates and oxalic acid with a molar ratio of total metal ions: oxalic acid of 1:1.1 was milled at room temperature for 5 h in a polyethylene container using zirconia balls as milling medium with a small amount of ethanol as the dispersion agent. The as-prepared mixed oxalate was then calcined at 800 °C in air for 4 h. The as-obtained powders were blended with an organic binder (PVA, $n = 1750$, Shanghai Chemical Reagent Co. Ltd., China) and sieved. Disk-shaped powder compacts of diameter 5 mm and thickness 3 mm were formed by uniaxial pressing at 60 MPa followed by isostatically pressing at 300 MPa. The powder compacts were heated in air to 400 °C at a rate of 100 °C/h and kept at that temperature for 2 h to remove the organic binder, and heated to 1050 °C at a rate of 120 °C/h and kept at that temperature for 4 h for sintering, and then furnace-cooled to room temperature.

The densification behavior of the powder was studied with a dilatometer (Netzsch DIL 402C, Germany) in an air flow at a heating rate of 5 °C/min using a cylindrical powder compact of length 1 cm and diameter 0.5 cm.

The calcined oxide powder and sintered ceramics were analyzed using XRD with a Philips X-Pert diffractometer using Cu Kα radition ($\lambda = 0.15418$ nm). (In order to ensure that the sintered ceramics for XRD analysis had the same thermal history as those for electrical measurements, they were heat treated at 850 °C in air for 20 min.) The lattice parameters were fitted by the Powdercell software using the least squares method. The density ρ was measured using Archimedes method in mercury. The relative density ρ_{rel} was determined according to the formula $\rho_{rel} = \rho/\rho_{th}$, where ρ_{th} is the theoretical density calculated from the lattice parameter as obtained from the XRD result.

X-ray photoelectron (XPS) spectra were acquired with a VG ESCALAB MK II spectrometer using Al Kα radiation. The residual pressure in the ion-pumped analysis chamber was maintained below 5×10^{-10} mbar during data acquisition. The binding energies (BE) were referenced to the C 1s peak at 285 eV. The microstructures of the sintered ceramics were observed with a Hitachi X-600 scanning electron microscope (SEM).

For measuring the electrical resistance, the two opposite sides of the sintered disks were polished and coated with platinum paste, heated at 850 °C for metallization and quenched to room temperature. Silver wires were attached as electrode leads. The electrical resistances were measured at 25 and 50 °C by a two-probe technique with an Agilent34401A digital multimeter. The thermal constant B was calculated according to the formula $B = 3853.89 \ln(R_{25}/R_{50})$, in which R_{25} and R_{50} are the resistances at 25 and 50 °C, respectively. After these measurements, the samples were tested for aging by keeping them in an oven at 150 °C in air for 1000 h. Aging is defined by $\Delta R/R_0 = (R - R_0)/R_0$, in which R_0 is the resistivity at 25 °C before the aging test, and R is the resistivity at 25 °C after the aging test.

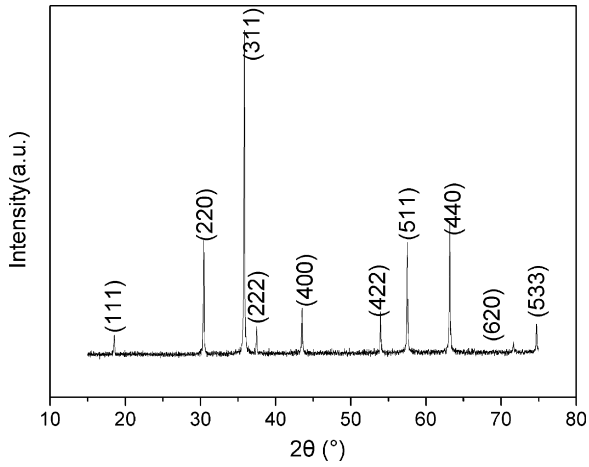

Fig. 1. XRD patterns of $Cu_{0.2}Zn_{1.0}Ni_{0.5}Mn_{1.3}O_4$ powders calcined at 800 °C in air.

3. Result and discussion

3.1. Preparation of powders and ceramics

XRD analysis shows that a single-phase oxide of spinel structure has been formed after calcination of the mixed oxalates at a relatively low temperature of 800 °C in air (Fig. 1). Fig. 2 presents the dilatometer curves of a compact of the as-prepared

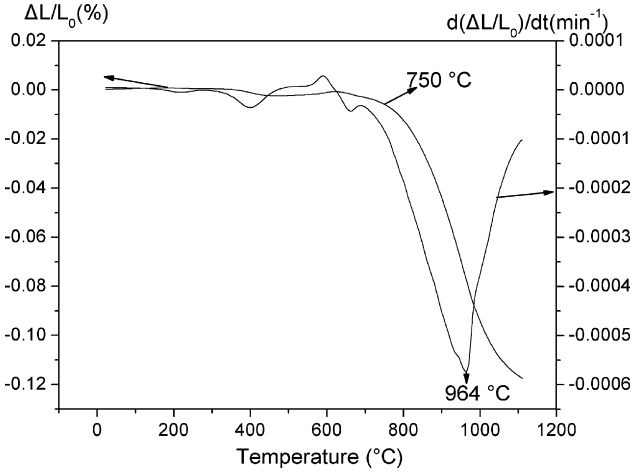

Fig. 2. Dilatometric curves of $Cu_{0.2}$ $Zn_{1.0}Ni_{0.5}Mn_{1.3}O_4$ measured at a heating of 5 °C/min in air.

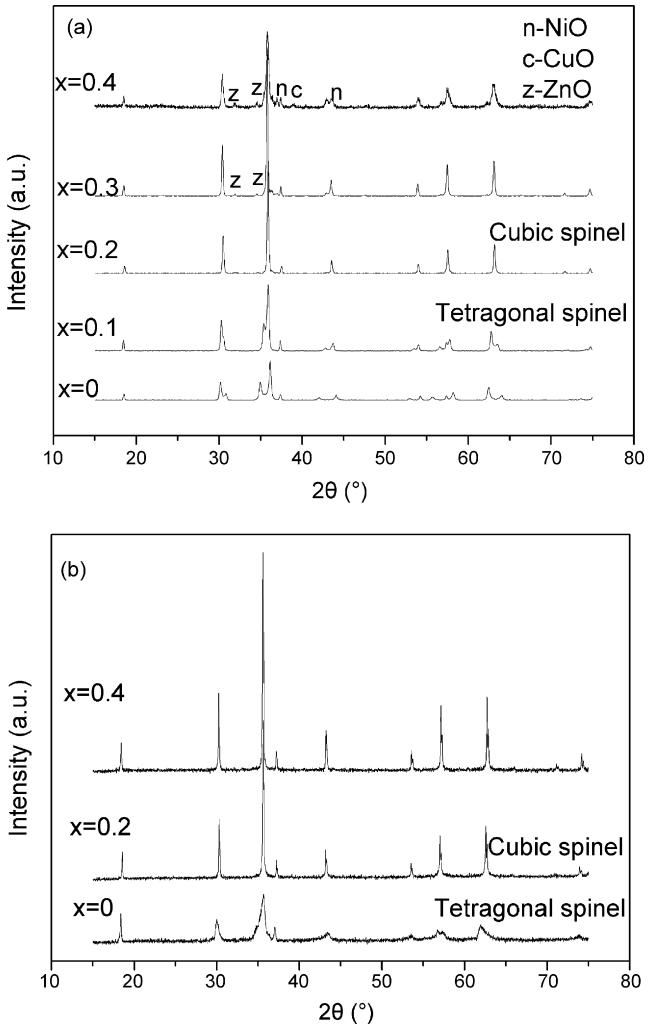

Fig. 3. XRD patterns of sintered ceramics (a) $Cu_xZn_{1.0}Ni_{0.5}Mn_{1.5-x}O_4$ and (b) $Cu_xNi_{0.5}Mn_{2.5-x}O_4$.

powder $Cu_{0.2}Zn_{1.0}Ni_{0.5}Mn_{1.3}O_4$. It can be seen that the densification starts to occur at ~750 °C, and a maximum shrinkage rate is attained at 965 °C at which the linear shrinkage of the compact is about 7.7%. For both compacts $Cu_xZn_{1.0}Ni_{0.5}Mn_{1.5-x}O_4$ and $Cu_xNi_{0.5}Mn_{2.5-x}O_4$, an isothermal sintering temperature of 1050 °C was chosen, which is about 100 °C higher than the temperature of maximum shrinkage. After sintering at that temperature for 4 h, a relative density over 95% was obtained for all ceramics.

3.2. Structure and cation distribution over the spinel lattice

Fig. 3 gives the powder XRD patterns of sintered ceramics $Zn_{1.0}Cu_xNi_{0.5}Mn_{1.5-x}O_4$ and $Cu_xNi_{0.5}Mn_{2.5-x}O_4$. For $Zn_{1.0}Cu_xNi_{0.5}Mn_{1.5-x}O_4$, a tetragonal distorted spinel structure is formed at a low Cu content ($x \leq 0.1$), and a cubic spinel structure at a higher x of 0.2. ZnO starts to appear at x of 0.3, and NiO and CuO also show up at x of 0.4. As to $Cu_xNi_{0.5}Mn_{2.5-x}O_4$, a tetragonal distorted spinel structure is also formed at low Cu content, which is also transformed to the cubic structure at higher Cu content. The as-observed phase transformation is attributed to the Jahn-Teller effect which is induced by the Mn^{3+} at the B-sites.[7] With increasing Cu content x, the concentration of Mn^{3+} is decreased and thus the Jahn-Teller effect becomes less pronounced, resulting in transformation from the tetragonal to cubic structure.

Fig. 4 presents the $Cu2p_{3/2}$ XPS spectra. With XPS, it is possible to distinguish between Cu ions at the A- and B-sites in the spinel. For the binding energy in the $Cu2p_{3/2}$ region, the following sequence is established: $Cu^{2+}(A) > Cu^{2+}(B) > Cu^{+}(A) > Cu^{+}(B)$.[8] Previous studies on Cu-doped manganite spinels showed that the peak at 930.7 eV could be assigned to $Cu^{+}(A)$, the peak at 933.0 eV to $Cu^{2+}(B)$ and the peak at 934.9 eV to $Cu^{2+}(A)$.[9,10] The XPS spectra shown in Fig. 4 are de-convoluted and assigned. For the Cu and Zn co-doped system $Zn_{1.0}Cu_xNi_{0.5}Mn_{1.5-x}O_4$, at x of 0.2, a large peak appears at 933.6 eV, which is assigned to $Cu^{2+}(B)$, and a small peak may be present at 930.8 eV, which corresponds to $Cu^{+}(A)$. Note that the intensity of the former is 95.8%, much stronger than that of the latter (4.2%), revealing that the majority of Cu ions exist as $Cu^{2+}(B)$. At a higher x of 0.4, only one peak exists at 934.2 eV, indicating that all the Cu ions now have converted to Cu^{2+}. But for the Zn-free system $Cu_xNi_{0.5}Mn_{2.5-x}O_4$, three peaks with comparable intensity are observed. Unlike the Cu and Zn co-doped system, the Cu ions now can take various valence and positions (see Table 1). Peak 1 (~931 eV) is assigned to $Cu^{+}(A)$, peak 2 to $Cu^{2+}(B)$, and peak 3 (934.7 eV) to $Cu^{2+}(A)$.

The site occupancy is of vital importance to the understanding of the electrical properties and the stability of the spinel-structured oxides. And numerous studies have been conducted regarding the distribution of Ni, Mn and Zn in the spinel oxides.[11] From these studies and the XPS analysis presented above, we propose a cation distribution of $(Zn_{1-a}{}^{2+}Cu_a{}^{+})_A[Zn_a{}^{2+}Cu_{x-a}{}^{2+}Ni_{0.5}{}^{2+}Mn_{0.5+a+x}{}^{4+}Mn_{1-a-2x}{}^{3+}]_BO_4{}^{2-}$ ($a \leq 0.01$) for $Zn_{1.0}Cu_xNi_{0.5}Mn_{1.5-x}O_4$ system, and $(Mn_{1.0-a-b}{}^{2+}Cu_a{}^{+}Cu_b{}^{2+})_A[Cu_{x-a-b}{}^{2+}Ni_{0.5}{}^{2+}Mn_{0.5-b+x}{}^{4+}Mn_{1+a+2b-2x}{}^{3+}]_BO_4{}^{2-}$ for the Zn-free system $Cu_xNi_{0.5}Mn_{2.5}O_4$, in which $a = 0.09$ and $b = 0.07$ at x of 0.2 and $a = 0.20$ and $b = 0.12$ at x of 0.4.

The electron microscope images of $Cu_{0.4}Ni_{0.5}Mn_{2.1}O_4$ and $Zn_{1.0}Cu_{0.4}Ni_{0.5}Mn_{1.1}O_4$ ceramics are shown in Fig. 5. In comparison with the Cu and Zn co-doped sample, $Cu_{0.4}Ni_{0.5}Mn_{2.1}O_4$ contains large (closed) pores. Previous studies have shown that Cu^{2+} in solid state can be easily reduced to Cu^{+} at temperatures above 1050 °C in air.[12] And the reduction of Cu^{2+} to Cu^{+} leads to the emission of O_2, leaving pores in the ceramics. However, for the Cu and Zn co-doped system, the reduction reaction is retarded, because the A-sites preferred for the Cu^{+} ions have been almost exclusively occupied by the Zn^{2+} ions.

3.3. Electrical properties

Fig. 6 shows the specific resistivity of $Cu_xZn_{1.0}Ni_{0.5}Mn_{1.5-x}O_4$ and $Cu_xNi_{0.5}Mn_{2.5-x}O_4$ measured at 25 °C. It can be seen that the resistivity for $Cu_xZn_{1.0}Ni_{0.5}Mn_{1.5-x}O_4$ decreases

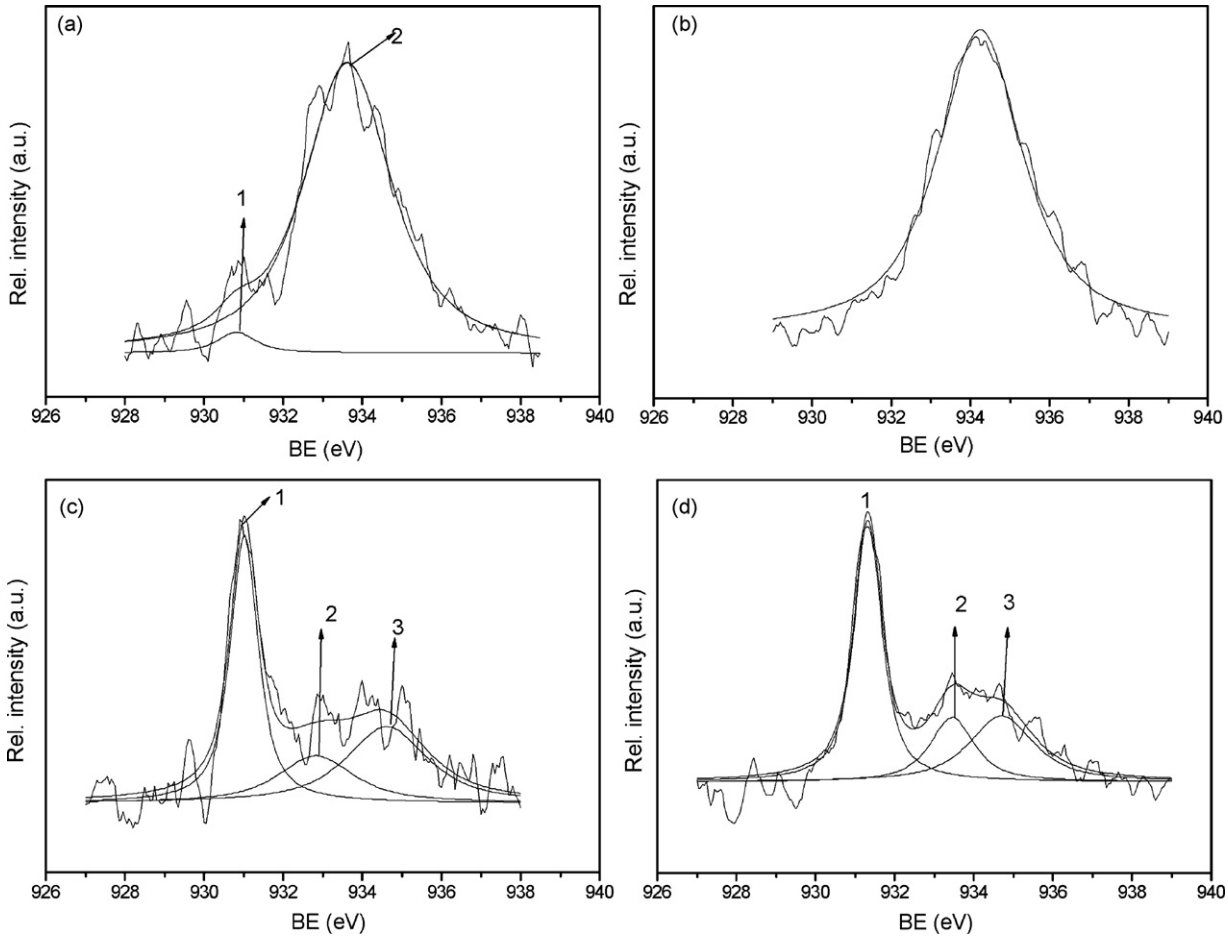

Fig. 4. XPS spectra in the Cu2p$_{3/2}$ region of (a) $Cu_{0.2}Zn_{1.0}Ni_{0.5}Mn_{1.3}O_4$, (b) $Cu_{0.4}Zn_{1.0}Ni_{0.5}Mn_{1.1}O_4$, (c) $Cu_{0.2}Ni_{0.5}Mn_{2.3}O_4$, and (d) $Cu_{0.4}Ni_{0.5}Mn_{2.1}O_4$.

from 3216 Ω cm to 1049 Ω cm with increasing Cu content x from 0 to 0.1, and then changes much less drastically with further increase in x. In contrast, the system doped with Cu alone shows a much sharper change in the resistivity. Its resistivity is 2907 Ω cm at x of 0, and 12.6 Ω cm at x of 0.4.

Fig. 7 gives the thermal constant B for these two systems. Clearly, B decreases slightly with increasing x for the Cu and Zn co-doped system. Its value is 3891 K at x of 0, and 3590 K at higher x of 0.4. As to the system doped with Cu alone, the change in B is much more pronounced. It takes a value of 3970 K at x of 0, and 2760 K at x of 0.4.

It is generally accepted that electrical conduction in nickel manganite spinel is via hopping of electrons between the Mn^{3+} and Mn^{4+} ions at the B-sites. According to this mechanism, the electrical resistivity ρ of the material is inversely proportional to the concentration product of Mn^{3+} and Mn^{4+}.[1] According to the cationic distributions given in the previous section of this paper, $[Mn^{3+}][Mn^{4+}]$ takes a value of 0.419 for $Cu_{0.2}Zn_{1.0}Ni_{0.5}Mn_{1.3}O_4$ and 0.523 for $Cu_{0.2}Ni_{0.5}Mn_{2.3}O_4$. Obviously, the small difference in the concentration product between these two systems can not account for their large difference in electrical resistivity, and thus there must exist some other electrical conduction mechanism. It has been suggested by Elbadraoui et al. that electron conduction may also proceed via jumping between Mn^{3+} and Mn^{4+} ions on more distant B-sites through Cu^+ and Cu^{2+} ions at the A-sites.[1] Therefore, we speculate here that the difference in the distribution of Cu ions between the Zn-containing and Zn-free systems is responsible for the

Table 1
Analysis of the Cu2p$_{3/2}$ XPS spectra of $Cu_xNi_{0.5}Mn_{2.5-x}O_4$

Sample	Peak 1 (Cu^+(A))		Peak 2 (Cu^{2+}(B))		Peak 3 (Cu^{2+}(A))	
	E (±0.1 eV)	I (±0.5%)	E (±0.1 eV)	I (±0.5%)	E (±0.1 eV)	I (±0.5%)
$Cu_{0.2}Ni_{0.5}Mn_{2.3}O_4$[a]	931.0	43.6	932.8	20.7	934.7	35.7
$Cu_{0.4}Ni_{0.5}Mn_{2.1}O_4$[a]	931.3	50.7	933.5	19.7	934.7	29.6
$Cu_{0.4}Ni_{0.5}Mn_{2.1}O_4$[b]	931.3	43.9	933.9	30.5	934.8	25.6

[a] As-prepared.
[b] After annealing at 150 °C in air for 1000 h.

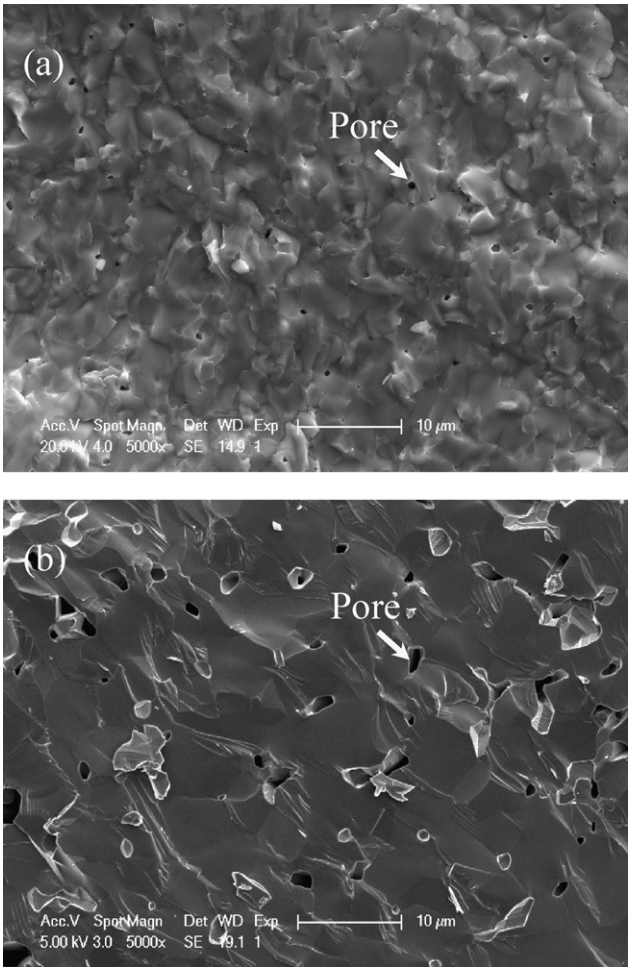

Fig. 5. SEM images of (a) $Cu_{0.4}Zn_{1.0}Ni_{0.5}Mn_{1.1}O_4$ and (b) $Cu_{0.4}Ni_{0.5}Mn_{2.1}O_4$ ceramics.

difference in their electrical properties, and further research is needed in this regard.

Fig. 8 shows the resistivity drift for $Cu_xZn_{1.0}Ni_{0.5}Mn_{1.5-x}O_4$ and $Cu_xNi_{0.5}Mn_{2.5-x}O_4$ after annealing at 150 °C in air for 1000 h. It can be seen that the drift is less than 2.6% for the

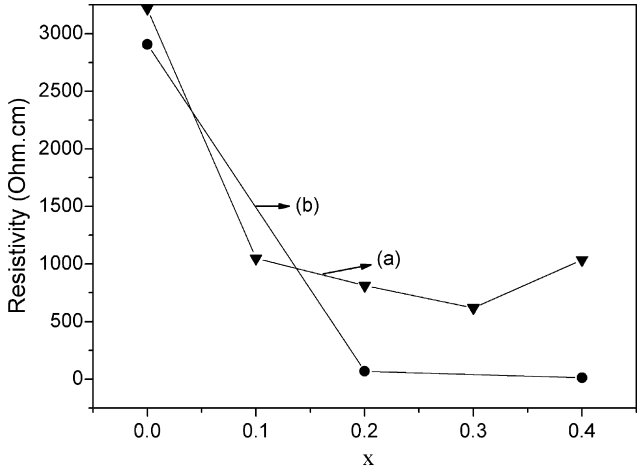

Fig. 6. Electrical resistivity of (a) $Cu_xZn_{1.0}Ni_{0.5}Mn_{1.5-x}O_4$ and (b) $Cu_xNi_{0.5}Mn_{2.5-x}O_4$.

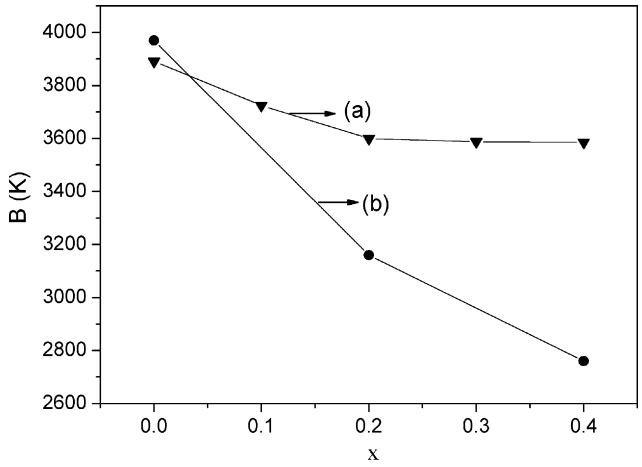

Fig. 7. Thermal constant B for (a) $Cu_xZn_{1.0}Ni_{0.5}Mn_{1.5-x}O_4$ and (b) $Cu_xNi_{0.5}Mn_{2.5-x}O_4$.

Cu and Zn co-doped system, but it is much larger for the system doped with Cu alone. It has been reported that Cu^+ ions at the A-sites are oxidized to Cu^{2+} ions by the atmospheric oxygen at temperatures below ~300 °C, which is followed by the migration of Cu ions from the A to the B-sites.[13] In the present study, the oxidation reaction is also verified by the XPS analysis on $Cu_{0.4}Ni_{0.5}Mn_{2.1}O_4$. It can be seen clearly that annealing at 150 °C has led to a significant decrease in the number of Cu^+ ions at the A-sites and to an increase in the number of Cu^{2+} ions at the B-sites (Table 1 and Fig. 9). These changes in the valence and site occupancy of the cations certainly will affect the electrical properties of the materials. For the Zn-doped system, due to the (almost) exclusive occupation of Zn^{2+} ions at the A-sites, the majority of Cu ions reside at the B-sites and these ions have a fixed valence of 2+. The invariability of the valence and site occupation of the Cu ions is likely to be largely responsible for the electrical stability of the Zn-containing system. Moreover, the Zn-doped material does not contain the large pores of the Zn-free material (see Fig. 5), thus the adsorption of atmospheric oxygen and subsequent oxidation of Cu^+ ions is retarded.

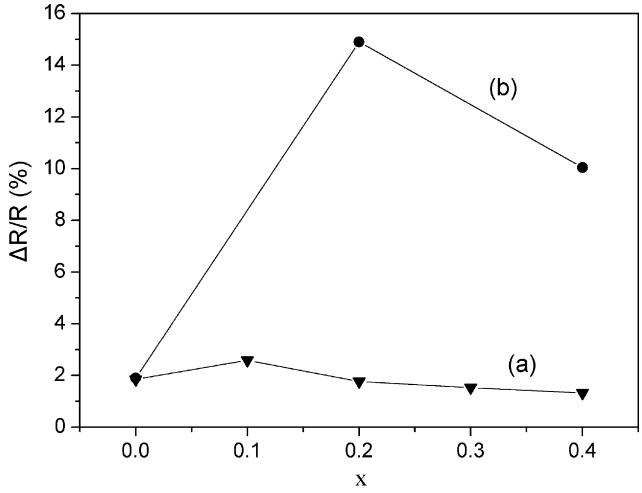

Fig. 8. Resistivity drifts of (a) $Cu_xZn_{1.0}Ni_{0.5}Mn_{1.5-x}O_4$ and (b) $Cu_xNi_{0.5}Mn_{2.5-x}O_4$.

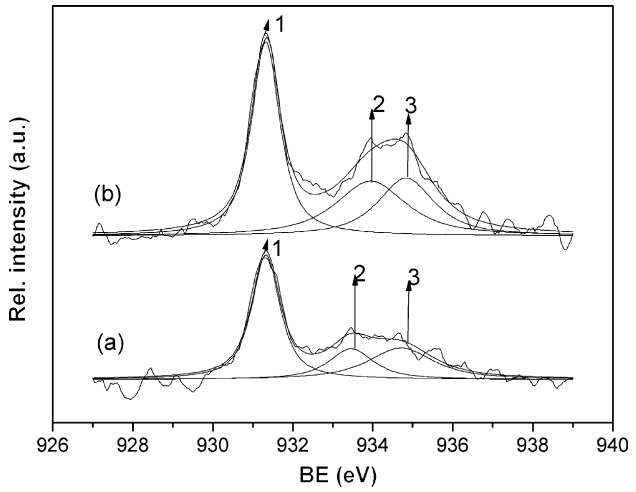

Fig. 9. XPS spectra in the $Cu2p_{3/2}$ region of $Cu_{0.4}Ni_{0.5}Mn_{2.1}O_4$ measured (a) before and (b) after annealing at 150 °C in air for 1000 h.

4. Conclusion

Dense Cu and Zn co-doped $Ni_{0.5}Mn_{2.5}O_4$ spinel-structured ceramics have been prepared from mixed oxalate-derived powder. Doping with both Cu and Zn in $Ni_{0.5}Mn_{2.5}O_4$ leads to a distribution of cations in which Zn ions occupy the A-sites, forcing the Cu ions to reside predominantly at the B-sites. The co-doped material exhibits a reduced electrical resistivity without much decrease in the thermal constant. In comparison with the material doped with Cu alone, the co-doped material also shows much improved electrical stability upon annealing at elevated temperature of 150 °C in air, which is attributed to the more stable distribution of cations in the spinel.

Acknowledgement

This work was supported by National Science Foundation of China (Grant No. 50225208).

References

1. E1badraoui, E., Baudour, J. L., Bouree, F., Gillot, B., Fritsch, S. and Rousset, A., Cation distribution and mechanism of electrical conduction in nickel–copper manganite spinels. *Solid State Ionics*, 1997, **93**, 219–225.
2. Fang, D. L., Wang, Z. B., Yang, P. H., Liu, W. and Chen, C. S., Preparation of ultra-fine nickel manganite powders and ceramics by a solid-state coordination reaction. *J. Am. Ceram. Soc.*, 2006, **89**, 230–235.
3. Wang, Z. B., Zhao, C. H., Yang, P. H., Winnubst, A. J. A. and Chen, C. S., X-ray diffraction and infrared spectra studies of $Fe_xMn_{2.34-x}Ni_{0.66}O_4$ ($0 < x < 1$) NTC ceramics. *J. Eur. Ceram. Soc.*, 2006, **26**, 2833–2837.
4. Metz, R., Electrical properties of N.T.C. thermistors made of manganite ceramics of general spinel structure: $Mn_{3-x-x'}M_xN_{x'}O_4$ ($0 \le x+x' \le 1$; M and N being Ni, Co or Cu). Aging phenomenon study. *J. Mater. Sci.*, 2000, **35**, 4705–4711.
5. Legros, R., Metz, R. and Rousset, A., The preparation, characterization and electrical properties of electroceramics made of copper–cobalt manganite spinel: $Mn_{2.6-x}Co_{0.4}Cu_xO_4$, $0 \le x \le 1$. *J. Eur. Ceram. Soc.*, 1995, **15**, 463–468.
6. Chanel, C., Guillemet-Fritsch, S., Sarrias, J. and Rousset, A., Microstructure and electrical properties of Ni–Zn manganite ceramics. *Int. J. Inorg. Mater.*, 2000, **2**, 241–247.
7. Malavasi, L., Ghigna, P., Chiodelli, G., Maggi, G. and Flor, G., Structural and transport properties of $Mg_{1-x}Mn_xMn_2O_{4\pm\delta}$ spinels. *J. Solid State Chem.*, 2002, **166**, 171–176.
8. Drouet, C., Laberty, C., Fierro, J. L. G., Alphonse, P. and Rousset, A., X-ray photoelectron spectroscopic study of non-stoichimetric nickel and nickel–copper spinel manganite. *Int. J. Inorg. Mater.*, 2000, **2**, 419–426.
9. Marco, J. F., Gancedo, J. R., Cong, H. N., Canto, M. del and Gautier, J. L., Characterization of $Cu_{1.4}Mn_{1.6}O_4$/PPy composite electrodes. *Solid State Ionics*, 2006, **177**, 1381–1388.
10. Fortunato, G., Oswald, H. R. and Reller, A., Spinel-type oxide catalysts for low temperature CO oxidation generated by use of an ultrasonic aerosol pyrolysis process. *J. Mater. Chem.*, 2001, **11**, 905–911.
11. Guillemet-Fritsch, S., Baudour, J. L., Chanel, C., Bouree, F. and Rousset, A., X-ray and neutron diffraction studies on nickel zinc manganite $Mn_{2.35-x}Ni_{0.65}Zn_xO_4$ powders. *Solid State Ionics*, 2000, **132**, 63–69.
12. Zhu, Y., Minura, K. and Isshiki, M., Oxidation mechanism of Cu_2O to CuO at 600–1050 °C. *Oxid. Met.*, 2004, **62**, 207–222.
13. Gillot, B., Buguet, S., Kester, E., Baubet, C. and Tailhades, Ph., Cation valencies and distribution in the spinels $Co_xCu_yMn_zFe_uO_{4+\delta}$ ($\delta \ge 0$) thin films studied by X-ray photoelectron spectroscopy. *Thin Solid Films*, 1999, **357**, 223–231.